



# Sodium metavanadate dispersed in Polyaniline composite matrix film for sensing application

T. Machappa<sup>1</sup> · S. Badrunnisa<sup>2</sup>

Received: 7 May 2021 / Accepted: 27 August 2021 / Published online: 9 September 2021  
© The Polymer Society, Taipei 2021

## Abstract

Composite of sodium metavanadate ( $\text{NaVO}_3$ ) and polyaniline (PANI) was formed by in-situ chemical polymerization in one step. Characterization techniques such as X-Ray diffraction, Scanning electron micrograph, and Fourier transform infra-red spectra confirm mixed phase of formation  $\text{NaVO}_3$  in PANI emeraldine salt. Conductivity decreases with an increase in wt of  $\text{NaVO}_3$  in PANI, the conductivity increases with temperature is due to an increase in disorderliness, induction of conformational changes within the composite, and thermally activated exponential behavior. The composites have shown high sensitivity in the low humidity range with the decrease in electrical resistance when exposed to humidity in the range of 20 to 50% RH. The moisture absorption is due to capillary condensation within the composite, which decreases the conductivity of the matrix with humidity. The transfer of charges from sensing material to analyte gas (donor) by penetration with enlargement of the polymer composites decreases the conductivity with the concentration of LPG.

**Keywords** Polyaniline · Sodium MetaVenadate · Conductivity · Humidity · Liquefied petroleum gas

## Introduction

For the past 31 years, ever since the discovery of conducting polymers by Alen MacDiarmid et.al, in 1980 has made significant attention for the researches due to their extensive variety of technical applications, such as electrical and electronic devices, rechargeable batteries, light-emitting devices, supercapacitors, humidity sensors and gas sensors [1–6]. Among the conducting polymers, polyaniline has the added advantage of its simple synthesis, doping, stability, and moderate conductivity has attracted much researches. In the past years, an extensive study on emerging cost-effective sensors for the monitoring toxic gases and humidity using inorganic semiconducting metal oxides such as tin oxide ( $\text{SnO}_2$ ), zinc oxide ( $\text{ZnO}$ ), titanium oxide ( $\text{TiO}_2$ ), Zinc

tungstate ( $\text{ZnWO}_4$ ), cadmium oxide ( $\text{CdO}_2$ ), Cerium oxide ( $\text{CeO}_2$ ) [7–9].

An accidental leaks of domestic liquefied petroleum gas (LPG) causes combustion accidents and a toxic CO gas combines with hemoglobin quickly resulting in human death, also they are potentially hazardous, the consistent and sensitive gas sensing instruments to increase the safety at home and industry is required. Detection of toxic and hazardous gas was started from early stages, most of the previous research focused on a new type of sensing materials where lack sensitivity, selectivity, and stability. Researchers have made their attention towards the study of sensing signal of the sensor material, the reports show that it is possible to distinguish different gases by measuring the features of sensor response [10]. Butane ( $\text{C}_4\text{H}_{10}$ ), Propane ( $\text{C}_3\text{H}_8$ ), butylenes ( $\text{C}_4\text{H}_8$ ), and propylene ( $\text{C}_3\text{H}_6$ ) are the normal constituents of the LPG, also it contains other similar gases in trace quantities, these are not chemically pure hydrocarbons but butane and propane are marked as quality products commercially. Researchers explored butane and propane but minimum work has been carried out on the LPG sensors. The earlier reports reveal, currently available sensors have two disadvantages low sensitivity and operating temperature is high, one has to compromise with any one of them. The high sensitive sensor works at a high temperature which increases the

✉ T. Machappa  
machappat@rediffmail.com

S. Badrunnisa  
badrunnisa.s@gmail.com

<sup>1</sup> Department of Physics, Ballari Institute of Technology and Management, Ballari 583 104, Karnataka, India

<sup>2</sup> Krupanidhi Degree College, Bangalore 560 035, Karnataka, India

power consumption and on the other side, low-temperature sensors are not sensitive enough to detect LPG at trace level [11–13].

For the past two and half decades conducting polymer composites are used in batteries, electrochromic devices, biosensors, etc. The derivatives of polyaniline are found well in humidity sensors, chemically synthesized PANI is considered as p-type doping, according to buildup model an unbounded electron pair on the nitrogen atom forms protonated. The nano-crystalline composites including ceramics and ceramic/conducting polymer are highly encouraging materials, which may be used for humidity and gas sensing applications because they exhibit improved sensing performance. Large surface areas are necessary for sensing, which can be obtained by highly-dispersed oxide particles. Large surface regions can provide high reaction contact between gas sensing materials and test gases. The standard structure of a metal oxide gas sensor is to have a porous structure for the large surface areas of interaction. The porous structure can be assembled by many small grains with empty spaces with pores among them. It is also indicated that a small grain size is suitable to improve the sensitivity [14–17].

The current report aims to study the electrical and sensing property of PANI and PANI / NaVO<sub>3</sub> composites for room temperature low humidity and LPG sensing.

## Experimental

### Synthesis

#### Pure polyaniline

5 ml Aniline is added to 200 ml of hydrochloric acid (0.1 M) to form aniline hydrochloride.  $14.6 \times 10^{-3}$  kg ammonium persulfate [(NH<sub>4</sub>)<sub>2</sub>S<sub>2</sub>O<sub>8</sub>] is dissolved in 300 ml of hydrochloric acid (0.1 M) to form ammonium per-sulfate hydrochloride. The polymerization of aniline is done by adding ammonium per-sulfate hydrochloride solution dropwise to aniline hydrochloride solution, with nonstop stirring for 6–8 h in the freezing mixture at 0–5 °C. The dark greenish precipitate of pure PANI was vacuum filtered, cleaned with deionized water, and to achieve constant weight the precipitate is dried for 24 h in the oven and achieved the yield of 3.2 to  $3.6 \times 10^{-3}$  kg per preparation of pure PANI [18].

#### Polyaniline/sodium metavanadate composite

5 ml Aniline is added to 200 ml of hydrochloric acid (0.1 M) mixed to have aniline hydrochloride and finely crushed sodium metavanadate (NaVO<sub>3</sub>) weight as 0.1 ( $0.34 \times 10^{-3}$  kg), this is against the average yield of PANI is mixed with aniline hydrochloride. The particle suspension

is confirmed by vigorous stirring using a magnetic stirrer. Aniline was polymerized in presence of NaVO<sub>3</sub> particles by drop-wise addition of  $14.6 \times 10^{-3}$  kg of ammonium persulfate [(NH<sub>4</sub>)<sub>2</sub>S<sub>2</sub>O<sub>8</sub>] dissolved in 300 ml of hydrochloric acid (0.1 M), with nonstop stirring for 6–8 h at 0–5 °C. The dark greenish precipitate of PANI/NaVO<sub>3</sub> composite was vacuum filtered, cleaned with deionized water, and dried for 24 h in the oven. The above procedure repeated for 0.2 ( $0.68 \times 10^{-3}$  kg), 0.3 ( $1.02 \times 10^{-3}$  kg), 0.4 ( $1.36 \times 10^{-3}$  kg) and 0.5 ( $1.7 \times 10^{-3}$  kg) weight NaVO<sub>3</sub>, the composite powder is stored in airtight container for further studies. [19].

### Characterization

The composites were used for the X-Ray diffraction (X-RD) studies to confirm retention of crystallinity and presence of NaVO<sub>3</sub> in PANI matrix using an X-ray diffractometer (Phillips—PW3710) with the source of radiation Cu K $\alpha$ . Fourier Transform Infra-Red (FTIR) spectra were recorded on a spectrophotometer (Perkin—Elmer 1600) in the medium of KBr for the confirmation of polymerization and composite formation along with pure PANI and NaVO<sub>3</sub>, the frequency peaks thus recorded of all three samples used for further analysis. The images of Scanning Electron Micrographs (SEM) images of pure PANI and PANI/NaVO<sub>3</sub> composite were taken on Environmental Scanning Electron Microscope (Phillips XL 30) to know the surface morphology of composite and distribution of NaVO<sub>3</sub> in pure PANI.

### Electrical conductivity

For the measurement of conductivity, the composite is pressed to have 10 mm diameter and 2 mm thickness pellets, these pellets were obtained by being subjected to a pressure of 98 k Pausing Universal testing machine (UTM-40). These pellets are provided by silver electrodes on both sides of the pellet with silver paste for temperature-dependent conductivity studies. Pellet sample was placed in temperature-controlled oven connected with Keithley multimeter (Model USA-2100) to record planar resistance of the composites and temperature-dependent electrical conductivity is calculated.

### Sensor studies

For sensor studies, PANI / NaVO<sub>3</sub> composite powder is sintered on an insulating substrate to form a film-like structure to expose the large surface area of the composite to test gas or humidity. Electrodes are provided at the two ends of a film with silver past for the measurement of planar resistance.

## Humidity sensor studies

PANI / NaVO<sub>3</sub> composite film was placed in the closed self-designed humidity sensor chamber of glass and planar resistance was recorded by High accuracy multimeter (Dot-tech). The humidity sensing studies were carried out by reducing the humidity to 20% RH by placing calcium chloride in a closed glass chamber and then humidity was increased steadily bypassing controlled water vapors into the chamber up to 50% RH. The planar resistance of the sensing composite in the chamber was recorded versus humidity from 20 to 50% RH at room temperature [20].

## Gas sensor studies

PANI / NaVO<sub>3</sub> composite film was placed in the closed self-designed gas sensor chamber of glass and connected to High accuracy multimeter (Dot-tech) to record planar resistance. The planar resistance of the composites was measured with reference environment air without test gas as initial resistance. Through the flow meter, the gas (LPG) was introduced into the sensor chamber with a rate of 25 ml/min by controlling the flow from the gas cylinder with a regulator. The planar resistance of PANI / NaVO<sub>3</sub> composite films in presence of test gas was measured every 20 s, such that 0.417 ml/sec gas flows into the chamber, slowly the gas concentration increases to 8.34 ml for every 20 s of the measurement. The change in resistance was calculated from the resistance of the composites with reference atmosphere air and the resistance of the composite in the presence of test gas (LPG) at regular intervals of time [21].

## Results and discussions

### X-Ray diffraction study (X-RD)

The X-RD diffraction pattern was recorded for all samples of PANI/NaVO<sub>3</sub> composites having the different weight of NaVO<sub>3</sub>, however X-RD pattern of PANI/ NaVO<sub>3</sub> composite having 0.5 wt of NaVO<sub>3</sub> is selected for the analysis as the concentration of NaVO<sub>3</sub> is more in 0.5 wt, because of which the intensity peaks will be high. The amorphous nature with micro-crystallinity of polyaniline was in Fig. 1a observed with a broad peak centered around  $2\theta \approx 27^\circ$  is in consistency with earlier reported data, maximum intensity peak at  $25.25^\circ$ .

The X-RD diffraction pattern of pure NaVO<sub>3</sub> reveals that, crystal structure as monoclinic (S.G: 12/a(15), PSC: mC20), having lattice parameters,  $a = 10.325 \text{ \AA}$ ,  $b = 9.468 \text{ \AA}$ ,  $c = 5.789 \text{ \AA}$  and  $\beta = 104.22^\circ$ . The prominent peaks  $2\theta = 18.73^\circ$ ,  $24.65^\circ$ ,  $32.08^\circ$ ,  $37.32^\circ$ ,  $41.41^\circ$ ,  $52.88^\circ$ ,  $63.27^\circ$  and  $68.11^\circ$  are from crystal planes (020), (021),

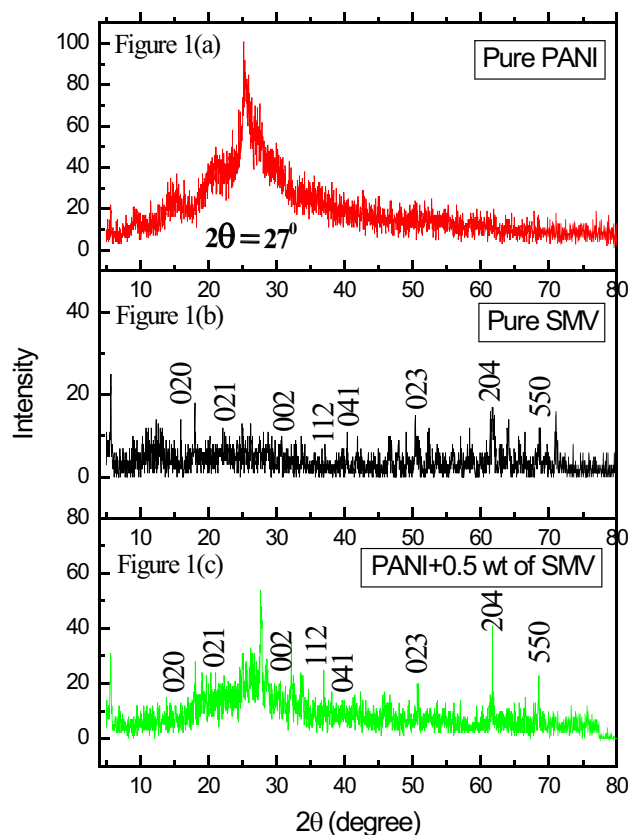


**Fig. 1** (a) X-RD pattern of pure PANI, (b) X-RD pattern of pure NaVO<sub>3</sub>, (c) X-RD pattern of PANI / NaVO<sub>3</sub> composite having 0.5 wt of NaVO<sub>3</sub> in PANI

(002), (112), (041), (023), (204) and (550) as shown in Fig. 1b. These peaks are confirmed from the reported standard data of JCPDS 70 – 1015 of NaVO<sub>3</sub>, equally Fig. 1c shows the amorphous nature of PANI with the monoclinic peak of NaVO<sub>3</sub> indicating the crystalline nature of the composite. X-RD pattern showing the same peaks in all cases when compared with the composite and pure NaVO<sub>3</sub> reveals NaVO<sub>3</sub> particle presence. This indicates that NaVO<sub>3</sub> has maintained its structure during the polymerization reaction and confirmed the distribution of NaVO<sub>3</sub> in PANI [22].

### Fourier Transform Infrared Spectra (FTIR)

The significant peaks observed in the case of FTIR spectra pure PANI (Fig. 2a), confirms the polymerization of monomer aniline into polymer polyaniline by the occurrence of spectral intensity peaks at  $3428 \times 10^{-2} \text{ m}^{-1}$  is due to N–H stretching,  $1625 \times 10^{-2} \text{ m}^{-1}$  is due to Benzenoid—Ring stretching,  $1563 \times 10^{-2} \text{ m}^{-1}$  is due to Quinoid—Ring stretching,  $1485 \times 10^{-2} \text{ m}^{-1}$  is due to C—C stretching + C=N stretching,  $1293 \times 10^{-2} \text{ m}^{-1}$  is due to CH bending + C—N stretching and  $1239 \times 10^{-2} \text{ m}^{-1}$  is due to C—C stretching + C—N stretching from FTIR spectrum

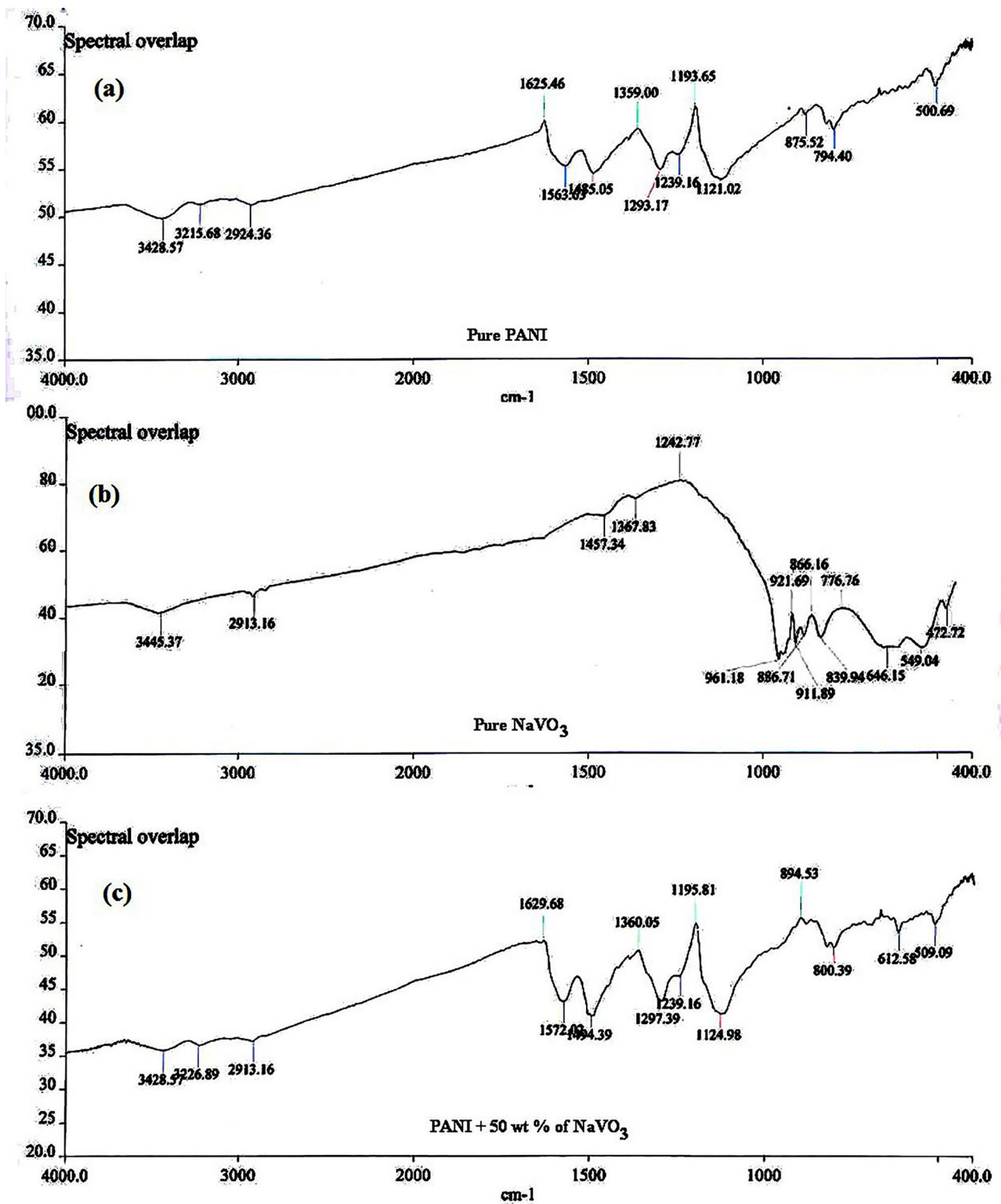


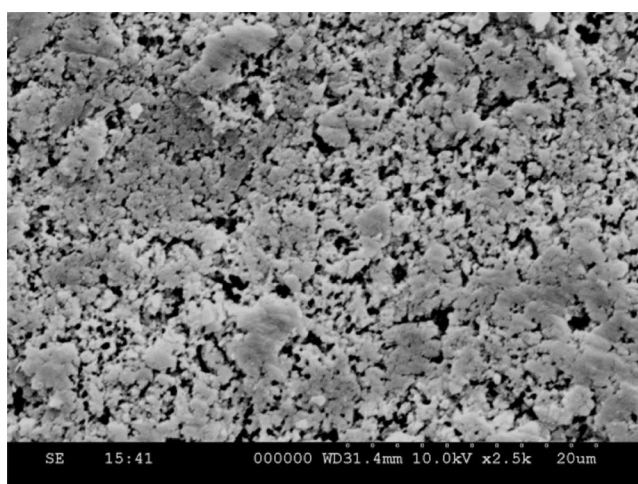
Fig. 2 (a) FTIR Spectra of pure PANI, (b) FTIR Spectra of pure NaVO<sub>3</sub>, (c) FTIR Spectra of PANI / NaVO<sub>3</sub> composite

of pristine PANI. The important spectral peaks of FTIR Spectra of pure  $\text{NaVO}_3$  (Fig. 2b) at  $776$  &  $549 \times 10^{-2} \text{ m}^{-1}$  of pristine  $\text{NaVO}_3$  are due to metal and oxygen bond stretching frequency. In FTIR Spectra of PANI/  $\text{NaVO}_3$  composite (Fig. 2c), the prominent spectral peaks observed at similar stretching frequencies are found in pristine PANI and pure  $\text{NaVO}_3$  spectra [23, 24]. The important intensity peaks observed in the case of pristine PANI, pristine  $\text{NaVO}_3$ , and PANI /  $\text{NaVO}_3$  composites are listed in Table 1 below. The comparison of stretching frequencies shows that the PANI /  $\text{NaVO}_3$  composite stretching frequencies in the case of benzenoid—ring stretching and quinoid—ring stretching in the pristine PANI are more than those observed to the PANI /  $\text{NaVO}_3$  composite, here these frequencies are moved little towards higher frequency side in the formation of

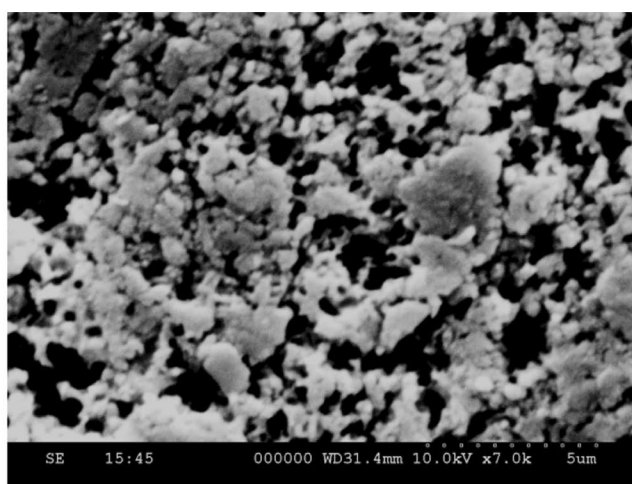
composite, this confirms the weak bond (Vander wall's) interaction between PANI Chain and  $\text{NaVO}_3$ . These results are consistent with earlier reported data in the literature [25].

### Scanning Electron Microscopy (SEM)

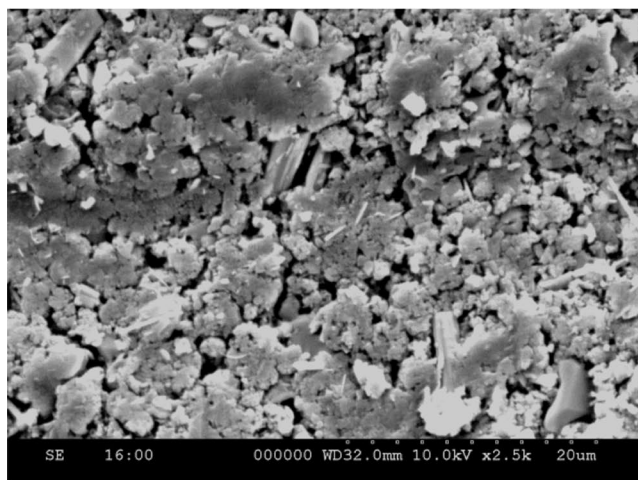
The pure PANI image of SEM shown in Fig. 3a, clearly shows a smooth and homogeneous structure. The presence of micro-crystalline structure distributed throughout can be seen and the presence of micro-crystalline structures in PANI is confirmed from X-RD studies, a granulated morphology with micro-crystalline structures is consistent with other reports. The SEM image of PANI/ $\text{NaVO}_3$  composite shown in Fig. 3c, possesses crystalline grains of  $\text{NaVO}_3$  in PANI matrix, further Fig. 3b, d shows the high-resolution



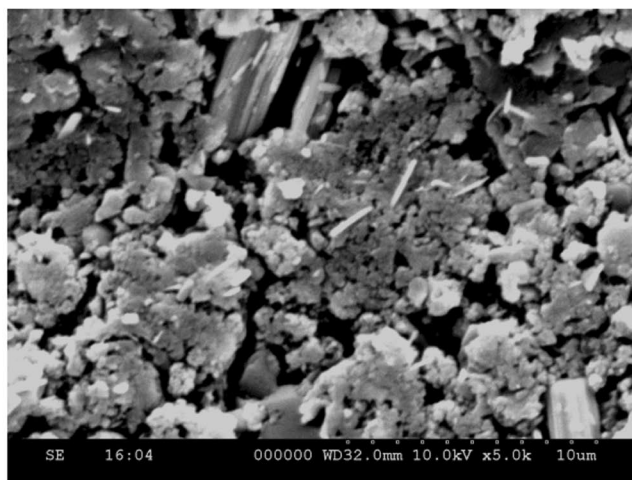
(a): 2.5 kV and 20  $\mu\text{m}$  SEM of pristine PANI



(b): 10 kV and 5  $\mu\text{m}$  SEM of pristine PAN



(c): 2.5 kV and 20  $\mu\text{m}$  SEM of PANI /  $\text{NaVO}_3$  composite



(d): 10 kV and 10  $\mu\text{m}$  SEM of PANI /  $\text{NaVO}_3$  composite

**Fig. 3** (a) 2.5 kV and 20  $\mu\text{m}$  SEM of pristine PANI, (b) 10 kV and 5  $\mu\text{m}$  SEM of pristine PAN, (c) 2.5 kV and 20  $\mu\text{m}$  SEM of PANI /  $\text{NaVO}_3$  composite, (d) 10 kV and 10  $\mu\text{m}$  SEM of PANI /  $\text{NaVO}_3$  composite

studies at 10 kV and 5  $\mu\text{m}$  and 10 kV and 10  $\mu\text{m}$  respectively, these images of SEM shows that the porous structure with capillary pores connected. Such a porous composite is possible to enable the adsorption of the vapors due to its large surface area available for interaction inside the capillary pores. The uniform spreading of  $\text{NaVO}_3$  micro-crystals in the PANI matrix was seen from SEM and also increase the porosity of the composite [26].

## Electrical conductivity

It is observed that the electrical conductivity increases as temperature increases in both PANI and PANI/ $\text{NaVO}_3$  composites as shown in Fig. 4a, b, this suggests that electrical conductivity is thermally activated. The change in conductivity is very low up to 110  $^\circ\text{C}$  in both PANI and PANI/ $\text{NaVO}_3$  composites, but it increases exponentially with the temperature above 110  $^\circ\text{C}$ . In conducting polymers the variation in electrical conductivity was explained by the Variable Range Hopping (VRH) model of Mott. According to Mott VRH-model, in non-metallic disordered materials like polymer composites and ceramics, the electron motion is specified by the thermally helped hopping of charge between localized states for electrons traps, these electron traps are distributed randomly within the

sample [27, 28]. The conductivity in non-metallic disordered materials is given by

$$\sigma(T) = \exp \left[ -\frac{T_0}{T^{\frac{1}{(n-1)}}} \right]$$

$$\text{where } T_0 = \frac{\lambda \alpha^3}{\rho_0 k}$$

where:  $\alpha$ —Coefficient of exponential decay of localized states,  $\rho_0$ —Density of states at Fermi level and  $\lambda$ —Dimensional constant. However, several simulations or models of conductivity predict that  $\sigma \propto T^{-0.5}$ .

In conducting polymers the increase in electrical conductivity depends on the conjugation length of the polymer chain, due to the phenomenon of the thermal curling effect, the conjugation length increase which leads to an increase in conductivity. On heating, the molecular arrangement makes the molecular conformation favorable for electron delocalization [29]. The conductivity of PANI /  $\text{NaVO}_3$  composites is more than that of pure PANI, which may be attributed to the percolation of PANI in presence of dispersed  $\text{NaVO}_3$  in the PANI matrix.

The variation of conductivity with wt of  $\text{NaVO}_3$  in PANI is shown in Fig. (5), the conductivity decreases as the

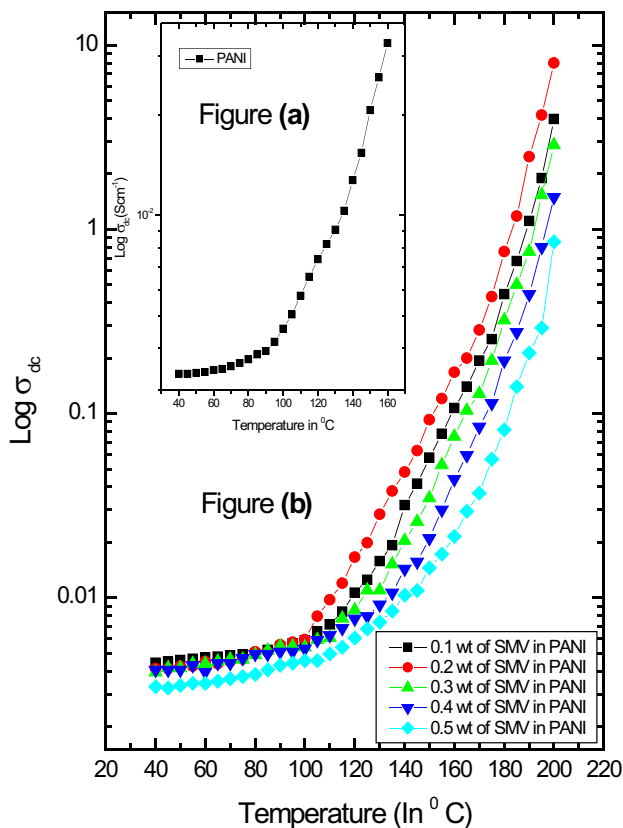


**Fig. 4** (a) Variation of  $\sigma_{dc}$  versus temperature Pure PANI, (b) Variation of  $\sigma_{dc}$  versus temperature PANI /  $\text{NaVO}_3$  composites

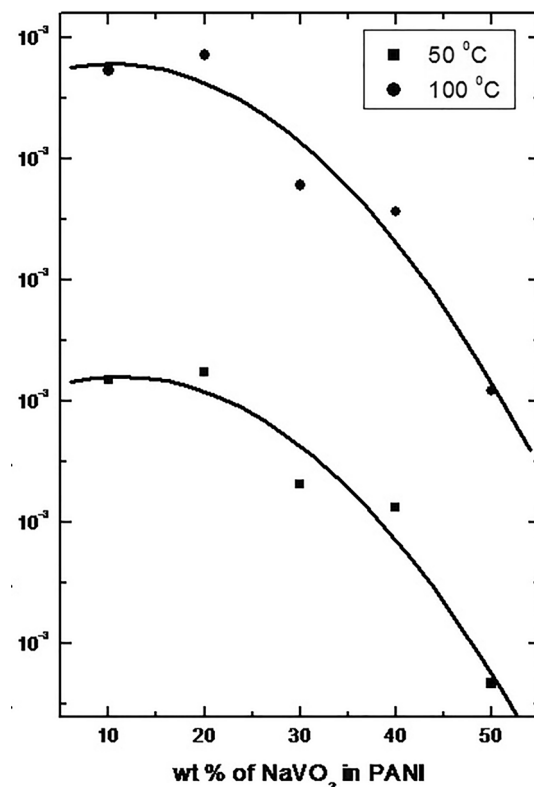


**Fig. 5** Variation of  $\sigma_{dc}$  versus wt of  $\text{NaVO}_3$  in PANI at two constant temperatures of 50  $^\circ\text{C}$  and 100  $^\circ\text{C}$

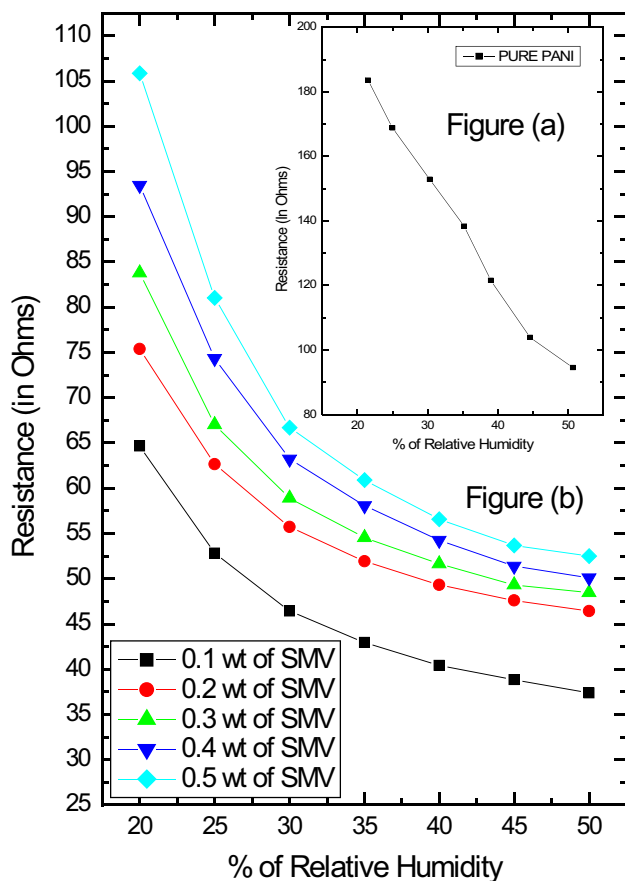


**Fig. 6** (a) Variations of resistance as versus % RH of Pure PANI, (b) Variations of resistance versus % RH of PANI / NaVO<sub>3</sub> composites

concentration of NaVO<sub>3</sub> increases in PANI. The disorderliness of composite is seen from X-RD and SEM data of these composites, the disorderliness will increase as wt of NaVO<sub>3</sub> increases in PANI, this disorderliness leads to reduce conformational charges in PANI. The decrease in conformational charges will reduce the order and delocalization length of the polymer chain, which reduce the conductivity.

The increase in conductivity depends on the hopping of charge carriers between localized sites, the hopping of charge carriers depends on polymer chain length, if chain length is extended then the charge carriers will have sufficient energy to hop hence conductivity increases, if the chain length reduces then charge carrier hopping is blocked then charge are unable to hop between localized sites hence decrease in conductivity [30]. In our study, it is found that extended chain length is observed in 0.2 wt of NaVO<sub>3</sub> in PANI, for all other composites reduction in chain length is observed. Hence increase in conductivity for only 0.2 wt of NaVO<sub>3</sub> in PANI was observed. The electrical conductivity of PANI/NaVO<sub>3</sub> composites is higher than that of pristine PANI, this increase in conductivity is due

to NaVO<sub>3</sub> molecules facilitate sufficient energy for hopping of charge carriers in the polymer chine.

### Humidity sensing study

The decrease in resistance with an increase in humidity was observed in both PANI and PANI / NaVO<sub>3</sub> composites as shown in Fig. 6a, b. This may be attributed to NaVO<sub>3</sub> ion mobility attached to polymer chain and the mobility of ions depends on humidity, the mobility increases as humidity increases, hence resistance decreases. Conducting polymer is coil up into compact form in dry conditions (low humidity) and the compact coil will uncoil into a straight-chain in wet conditions (high humidity). In conducting polymers this geometry of straight-chain is favorable to enhance the mobility of ions or enhance the transfer of charge carriers across the polymer chain, this charge transfer of charges and mobility of ions will reduce resistance and increase conductivity [31]. On the other hand, the conductivity depends on the condensation of water molecules in capillary pours within the sensing material, this pours structure will also cause the change in conductivity.

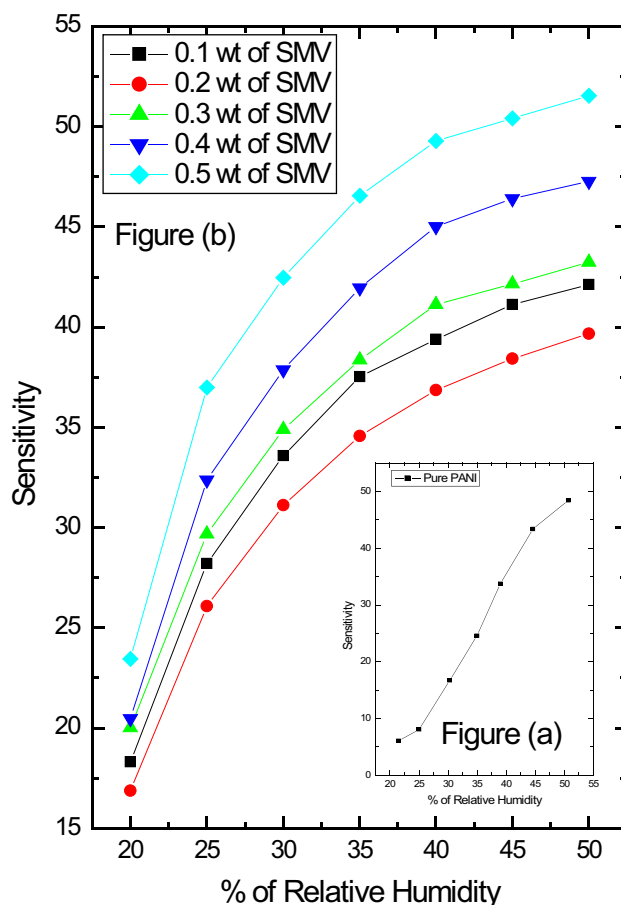


**Fig. 7** (a) Sensitivityverses humidity of pristine PANI, (b) Sensitivityverses humidity of PANI / NaVO<sub>3</sub> of composites

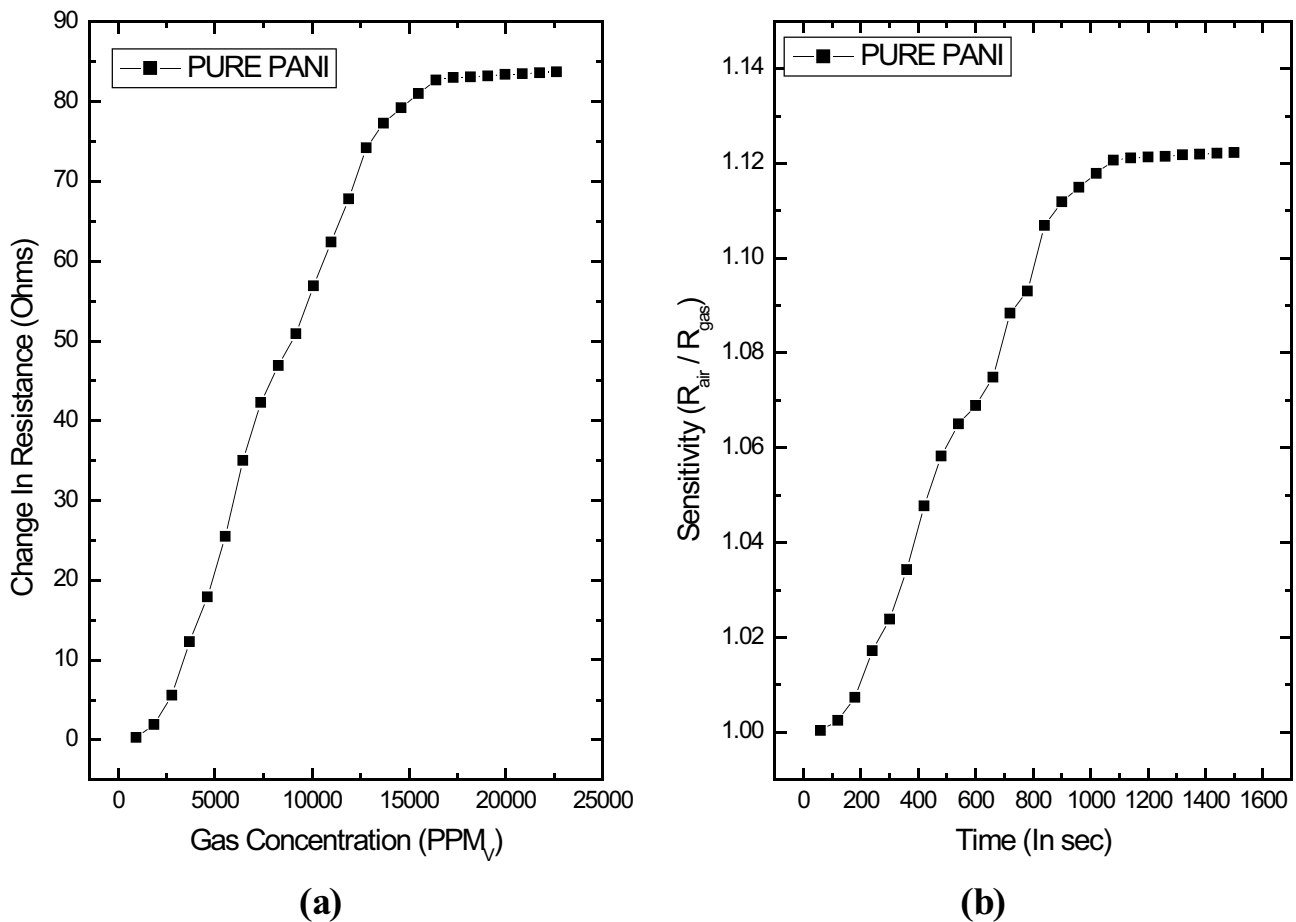


**Fig. 8** (a) Change in resistance versus concentration of LPG of pure PANI, (b) Sensitivity versus expose time of pure PANI to LPG

Humidity sensor performance characteristics such as sensitivity, reproducibility, time response, etc., will depend on its microstructure. These characteristics are determined by the specific interaction surface area between analyte and sensing materials, but the specific area of interaction depends on its porosity, as porosity increases the specific area of interaction also increases. SEM microstructure revealed the presence of capillary pores in PANI / NaVO<sub>3</sub> composite, thus the specific area of interaction is the principle microstructure for low humidity conditions. Therefore a definite correlation is established between the number of water molecules taken by the capillary pores and the resistance of the sensing material [32].

The sensitivity (*S*) of the sensing material in the detection of humidity is given by

$$S_H = \left| \frac{\text{Change in resistance}}{\text{Initial resistance}} \right| \times 100$$

Change in resistance is ( $RH_2 - RH_1$ ), where  $RH_1$  is the initial resistance of the sample and  $RH_2$  is the resistance at the next level of humidity, the next level of humidity depends on the measurement of resistance versus relative

humidity in the chamber. Figure 7 gives the variation of sensitivity with humidity and wt of NaVO<sub>3</sub> in PANI. In our study it is clear that sensitivity increases with an increase in humidity and follows an exponential growth, also the sensitivity increases as wt of NaVO<sub>3</sub> increases in PANI, it is a fund that at 40%RH the percentage of sensitivity is 36.85, 38.39, 41.12, 45.01 and 49.27 for 0.1, 0.2, 0.3, 0.4 and 0.5 wt of NaVO<sub>3</sub> in PANI respectively. The increase in sensitivity with an increase in wt of NaVO<sub>3</sub> is due to an increase in porosity of the composite, hence a large surface area available for the interaction of water vapors with the composite to have a considerable change in resistance.

### Gas sensing study

The change in resistance with the concentration of LPG in parts per million (PPM) at a constant volume of pure PANI is shown in Fig. 8a. The gas is made to flow at a constant rate of 25 ml/min into the sensing chamber. It is found that change in resistance increases with the concentration of gas. The change in resistance of pure PANI is due to absorption of the gas, this may be attributed



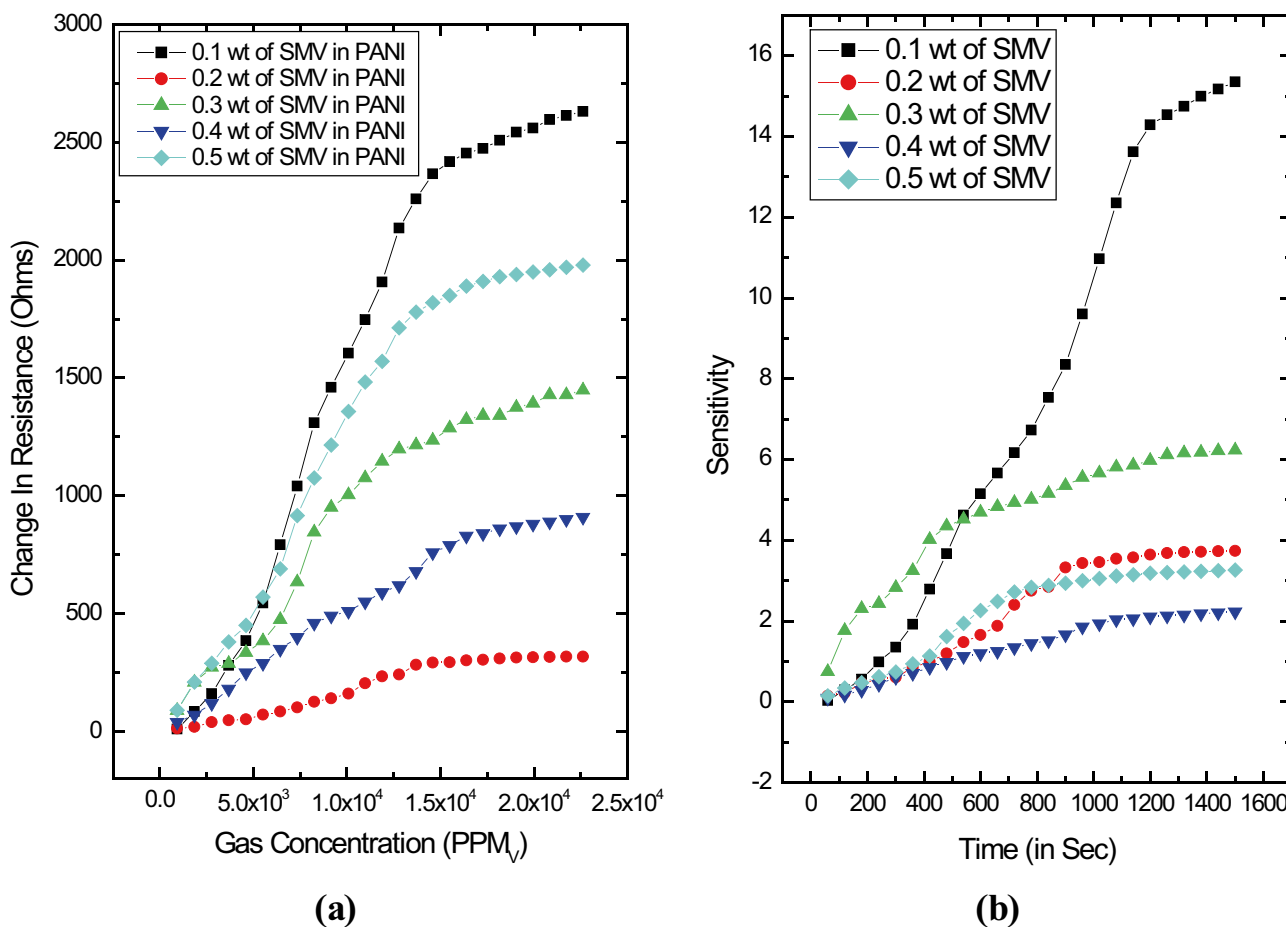


**Fig. 9** (a) Change in resistance versus concentration of LPG of PANI / NaVO<sub>3</sub> composites (b) Sensitivity versus expose time of composite to LPG

as a two-stage process. Firstly swelling of polymer matrix due to penetration of gas and secondly diffusion of gas into the swelled material with an increased rate of flow. In

this process, the transfer of charge carriers from sensing material to analyte gas molecules takes place, i.e. the charge exchange from sensing surface to test gas. The weak

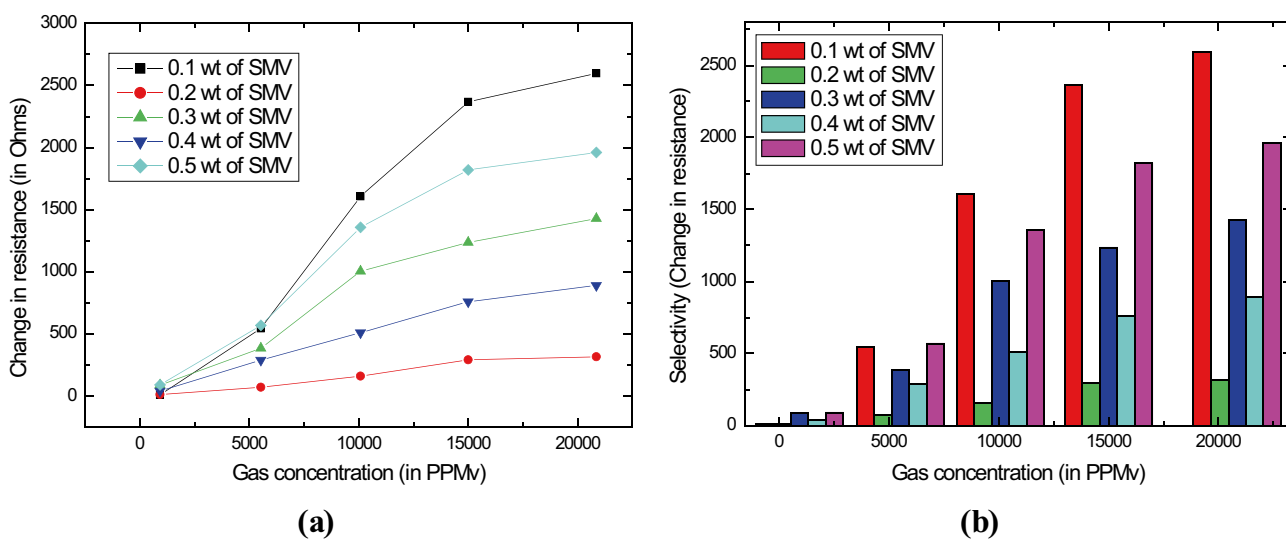


**Fig. 10** (a) Change in resistance versus gas concentration (b) Selectivity from the change in resistance versus gas concentration

**Table 1** Observed peaks of FTIR spectra with group assignments

Sample	Wave number ( $\times 10^{-2} \text{ m}^{-1}$ )	Assignment
Pure PANI	3428	N–H stretching
	1625	Benzenoid—Ring stretching
	1563	Quinoid—Ring stretching
	1485	C—C stretching + C=N stretching
	1293	CH bending + C-N stretching
	1239	C—C stretching + C-N stretching
Pure $\text{NaVO}_3$	776, 549	Metal oxygen stretching
PANI / $\text{NAaO}_3$ composite	3428	N–H stretching
	1629	Benzenoid—Ring stretching
	1572	Quinoid—Ring stretching
	1494	C—C stretching + C=N stretching
	1297	CH bending + C-N stretching
	1239	C—C stretching + C-N stretching
	894	PANI – $\text{NAVO}_3$
	800	Metal oxygen stretching
	612	Metal oxygen stretching

charge—transfer between the polymer matrix and test gas is responsible for the removal of charge, here the polymer matrix acts as donor, and test gas LPG act as an acceptor [33, 34]. The sensitivity of pure PANI is shown in Fig. 8b.

It is observed that the electrical resistance increases with the concentration of LPG for all five composites as in Fig. 9a. The variation of resistance of the composite depends on the type of doping material to PANI, dopants like metal oxides, bi-metal oxides, bio-materials, etc., The mechanism of gas sensing is explained in terms of variation in conductivity or variation in resistance of sensing materials, one is the absorption of atmospheric oxygen molecule on the sensing composite surface and other is the direct reaction with lattice / interstitial oxygen by test gas. The atmospheric oxygen absorbed on the composite surface will extract an electron from the sensing material and transfer it to the test gas and/or lattice / interstitial oxygen will interact to transfer the electron from sensing material to test gas, these are mostly accountable for the detection of test gases [35].

The sensing mechanism of swelling and surface charge transfer as explained earlier are responsible for the change

in resistance within the sensing material. From Fig. 9a it is clear that change in resistance has started from 30 s and is very rapid at low concentrations and saturates after 15.5 min.

The response of a gas sensor is a function of the concentration of the gas, in our study we have recorded resistance of the composite versus change in the concentration of gas in a closed sensor chamber. If  $R_a$  is the initial resistance of the composite in the air (no test gas) and  $R_g$  is the resistance of the composite in presence of the test gas (LPG) atmosphere, then the sensitivity of the gas is defined as the response of the sensor in presence of the test gas (LPG) to reference atmosphere (air) and is given by.

$$S_g = \left[ \frac{R_a}{R_g} \right]$$

Sensitivity is very high for 10 wt% of  $\text{NaVO}_3$  in PANI among all the composites as shown in Fig. 9b, the gas is introduced into the chamber is at a study rate of 25 ml/min, the composite response starts by changing its resistance instantaneously after the introduction of gas, the sensitivity of sensing composite is due to the presence of the large number of pores which is revealed by SEM, hence 0.1 wt of  $\text{NaVO}_3$  in PANI is highly sensitive to detect LPG. The.

It has been reported from our study, 0.1 wt of  $\text{NaVO}_3$  in PANI has shown the highest change in resistance among all the composites in the presence of test gas LPG as in Fig. 10a. The change in resistance for 925 PPMV (low concentration) is 10  $\Omega$ , but for 22,624 PPMV (high concentration) is 3.21 k $\Omega$ , for 0.5 wt of  $\text{NaVO}_3$  the change in resistance for 925 PPMV (low concentration) is 90  $\Omega$ , but for 22,624 PPMV (high concentration) is 1.98 k $\Omega$ . the difference of change in resistance from low concentration of LPG to high concentration is 3.2 k $\Omega$  and 1.89 k $\Omega$  for 0.1 and 0.5 wt. Among all five composites, 0.1 and 0.5 wt of  $\text{NaVO}_3$  in PANI have the highest sensitivity and selectivity with good response for LPG detection, Fig. 10b shows there is a large difference in resistance is sufficient to produce an electrical signal from the composite in presence of LPG with good resolution[36].

**Table 2** The performance of the detection of LPG of present work compared with the previous reports

SN	Composite	wt%	Resistance at Gas Concentration		Resistance Range (in Ohm)	Ref
			952 (in PPMv)	22,624(in PPMv)		
01	PANI / $\text{MgCrO}_4$	40 wt%	14.3	102	87.7	[21]
02	PANI / $\text{MgCrO}_4$	50 wt%	9.8	94	84.2	[21]
03	PANI / $\text{Sr}_3(\text{AsO}_4)_2$	20 wt%	54	1544	1490	[35]
04	PANI / $\text{Sr}_3(\text{AsO}_4)_2$	30 wt%	16	1077	1061	[35]
05	PANI / $\text{NaVO}_3$	10 wt%	10	3210	3200	Present work
06	PANI / $\text{NaVO}_3$	50 wt%	90	1980	1890	Present work

The sensing mechanism is either oxidation or reduction; that is an electron transfer from sensing material to gas decreases the resistance or gas to sensing material increases the resistance, which depends on the surface area of interaction. As the surface area of interaction increases, the sensitivity also increases, this surface area of interaction depends on porosity of the sensing material. In our study, we find that porosity is more for 0.1 and 0.5 wt of  $\text{NaVO}_3$  composites as revealed by SEM.

The performance of detection of LPG earlier reported composites are as shown in Table 2. We observe that the range of change in resistance in the present work is much more than the previous work, hence PANI /  $\text{NaVO}_3$  composite is a competent material for LPG sensing.

Thus the PANI /  $\text{NaVO}_3$  composites have high sensitivity towards the presence of LPG, hence it is found to be a promising composite for low humidity and LPG sensing material for the fabrication of sensor devices.

## Conclusions

Polyaniline and PANI /  $\text{NaVO}_3$  composites are synthesized by in situ chemical polymerization method. The XRD pattern confirms the monoclinic crystalline structure of  $\text{NaVO}_3$  and it has reserved its crystalline structure after it is distributed in the PANI matrix during the formation of the composite. FTIR spectra confirm the polymerization of aniline and PANI /  $\text{NaVO}_3$  composite, by showing metal–oxygen stretching frequency and moved towards higher frequency side, this is attributed to weak Vanderwall bond interaction between  $\text{NaVO}_3$  and polyaniline chain. SEM reveals that the distribution of crystalline grains of  $\text{NaVO}_3$  in PANI matrix, further the porous structure with capillary pores connected. Thermally activated dc-conductivity was observed, wherein conductivity increases with temperature for all the composites. The decrease in the conductivity with an increase in  $\text{NaVO}_3$  in the PANI matrix is attributed to the blocking of charge carriers hopping due to the reduced chain length polymer matrix. The decrease in the resistance with increasing humidity is due to the mobility of  $\text{NaVO}_3$  due to the capillary condensation of water molecules within the sensing material. The increase in resistance, hence decrease in conductivity with the concentration of LPG is due to the weak charge-transfer complex between the polymer matrix and test gas is responsible for charge removal, here the polymer matrix acts as a donor, and test gas LPG act as an acceptor. This sensors composite works at room temperature which is an added advantage over conventional ceramic sensors which work at elevated temperatures. The 0.1 and 0.5 wt of  $\text{NaVO}_3$  in PANI has shown the highest sensitivity and selectivity for the detection of LPG at room temperature.

## References

- Mac Diarmid AG, Chiang JC, Richter AF, Epstein AJ (1987) Polyaniline: A new concept in conducting polymers. *Synth Met* 18(1–3):285–290
- MacDiarmid AG, Yang LS, Huang WS, Humphrey BD (1987) Polyaniline: Electrochemistry and application to rechargeable batteries. *Synth Met* 18:393–398
- Machappa T, Ambika Prasad MVN (2009) Low-frequency AC conduction in Polyaniline / Zinc tungstate ( $\text{PANI}/\text{ZnWO}_4$ ) composite. *Ferroelectrics* 392:71–80
- Majunatha S, Machappa T, ASunilkumar, Y TRavikiran. (2018) Tungsten disulfide: An efficient material in the enhancement of AC conductivity and dielectric properties of polyaniline. *J Mater Sci Mater Electron* 29:11581–11590
- Sunilkumar A, Manjunatha S, Machappa T, Chethan B, Ravikiran YT (2019) A tungsten disulphide-Polypyrrol composite based – humidity sensor at room temperature. *Bullion of Materials Science* 42(271):1–5
- Khened BS, Machappa T, Ambika Prasad MVN, MSasikala, (2012) Studies on DC conductivity and LPG sensing behavior of PANI/ $\text{CeO}_2$  composite. *Int J Sci Res* 1(4):180–184
- Patil RC, Patil SF, Mulla IS, Vijayamohan K (2000) Effect of protonation media on chemically and electrochemically synthesized polyaniline. *Polym Int* 49:189–196
- Cantalini C, MPelino, (1992) Microstructure and humidity-sensing characteristics of  $\alpha\text{-Fe}_2\text{O}_3$  ceramic humidity sensors. *J Am Ceram Soc* 75:546–551
- Trivikrama Rao GS, Tarakarama Rao D (1999) Gas sensitivity of ZnO based thick film sensor to  $\text{NH}_3$  at room temperature. *Sens Actuators B* 55:166–169
- Nakata S, Takemur K, Neya K (2001) Non-linear dynamic responses of a semiconductor gas sensor: evaluation of kinetic parameters and competition effect on the sensor response. *Sens Actuators B* 76:436–441
- Khened BS, Machappa T, Pradeep MVN, Ambika Prasad MVN, Sasikala M (2016) Studies on LPG Sensing Property of Polyaniline /  $\text{BaZrO}_3$  Composites. *Mater Today: Proc* 3:369–375
- Srivastava A, Rashmi KJ (2007) Study on ZnO – doped tin oxide thick film gas sensors. *Mater Chem & Phys* 105:385–390
- Wagh MS, Jain GH, Patil DR, Patil DR (2007) Surface customization of  $\text{SnO}_2$  thick film using  $\text{RuO}_2$  as a surfactant for the LPG response. *Sens Actuators B* 122:357–364
- Scrosati B (1993) *Encyclopedia of polymer science and engineering* London: Chapman and Hall, Chapter 7
- Palmisano F, De Benedetto GE, Zamboni CG (1997) Lactate amperometric biosensor based on an electrosynthesized bilayer film with covalently immobilized enzyme. *Analyst* 122:365–369
- Bai H, Shi G (2007) Gas sensors based on conducting polymers. *Sensors* 7(3):267–307
- Lee CY, Lee GB (2005) Humidity Sensors: A Review. *Sens Lett* 3(1–4):1–15
- Majunatha S, Machappa T, Ravikiran YT, Chethan B, Sunilkumar A (2019) Polyaniline based stable humidity sensor operable at room temperature. *Phys Rev B Condens Matter* 561:170–178
- Sasikala M, Anilkumar KR, Prasad MA (2009) Humidity sensing behavior of polyaniline/strontium arsenate composite. *Sens Transducers* 107(8):77–85
- Machappa T, Anilkumar KR, Sasikala M, Prasad MA (2008) Design of sensor setup and study of humidity sensing behaviour of conducting polyaniline/ceramic composites. In 2008 3rd International Conference on Sensing Technology Nov 30–Des 3, (Tainan, Taiwan) 284–288
- Machappa T, Sasikala M, Prasad MA (2010) Design of Gas Sensor Setup and Study of Gas (LPG) Sensing Behavior of Conducting

- Polyaniline/Magnesium Chromate ( $\text{MgCrO}_4$ ). *IEEE Sensors Journal* 10(4):807–813
22. Manjunatha S, Sunilkumar A, Ravikiran YT, Machappa T (2019) Effect of holmium oxide on impedance and dielectric behavior of polyaniline - holmium oxide composite. *Journal of material science. Materials Electronics* 30:10332–10341
  23. Koenig JL (1999) *Spectroscopy of polymers*. Amsterdam: Elsevier, 2nd ed
  24. Pavia DL, Lampman GM, Kriz GS (2001) *Introduction to spectroscopy*. Fort Worth: Harcourt College Publishers, 3rd ed
  25. Machappa T, M V Nambika Prasad, (2009) AC Conductivity and Dielectric Behavior of Polyaniline / Sodium Metavanadate (PANI/  $\text{NaVO}_3$ ) Composites. *Phys B* 404(21):4168–4172
  26. Manjunatha S, Ravikiran YT, Chethan B, Devendrappa H, Machappa T (2020) Alternating current response studies on polyaniline – neodymium oxide composite. *AIP: Conference proceedings* 2244:08009:1–4
  27. Mott NF, Davis E (1979) *Electronic process in non-crystalline materials*. (ede) Clarendon press, Oxford
  28. Salunkhe RR, Shinde VR, Lokhande CD (2008) Liquefied petroleum gas (LPG) sensing properties of nanocrystalline CdO thin films prepared by chemical route: Effect of molarities of precursor solution. *Sensors and Actuators B* 133:296–301
  29. Kobayashi A, Ishikawa H, Amano K, Satoh M, Hasegawa E (1993) Electrical conductivity of annealed polyaniline. *J Appl Phys* 74(1):296–301
  30. Olmedo L, Chanteloube I, A Germain, M Petit, E M Genies, (1989) Characterization of electrochemically prepared conductive polymers by in-situ conductivity measurements. *Synth Met* 28(1–2):165–170
  31. Sunilkumar A, Manjunatha S, Chethan B, Ravikiran YT, Machappa T (2019) Polypyrrole–Tantalum disulfide composite: An efficient material for fabrication of room temperature operable humidity sensor. *Sensors and Actuators A* 298(111593):1–8
  32. Machappa T, Prasad MA (2012) Humidity sensing behaviour of polyaniline/magnesium chromate ( $\text{MgCrO}_4$ ) composite. *Bull Mater Sci* 35(1):75–81
  33. Roy AS, Anilkumar KR, Sasikala M, Machappa T, Prasad MV (2011) Sensitivity enhancement for LPG detection by employing cadmium oxide doped in nanocrystalline polyaniline. *Sens Lett* 9:1–7
  34. Hosseini SH, Abdi OS, Entezami AA (2005). Toxic gas and vapor detection by polyaniline gas sensors. *Iran Polym J (English)* 14(4(58)):333–344
  35. Machappa T, Badrunnisa S (2020) Strontium arsenate doped conducting polyaniline matrix as gas sensor. *In Journal of Physics: Conference Series* 1706(012015):1–7
  36. Roy AS, Machappa T, Prasad MA, Anilkumar KR (2011) Sensitivity and selectivity studies on polyaniline/molybdenum trioxide composites to liquid petroleum gas. *Sens Transducers* 125(2):220–228

**Publisher's Note** Springer Nature remains neutral with regard to jurisdictional claims in published maps and institutional affiliations.